Proceedings of the Estonian Academy of Sciences,
2023, **72**, 4, 371–381
https://doi.org/10.3176/proc.2023.4.02
Available online at www.eap.ee/proceedings

PHARMACOKINETICS

# Predictive modelling and simulation for taming the chance and luck in biologics drug discovery

Armin Sepp

Certara UK Ltd, Simcyp Division, 1 Concourse Way, Level 2-Acero, Sheffield S1 2BJ, United Kingdom; armin.sepp@certara.com

Received 9 January 2023, accepted 3 February 2023, available online 24 October 2023



**Abstract.** Three Pillars of Survival paradigm in the pharmaceutical drug discovery stipulates that a drug candidate is more likely to reach Phase III if it meets the following criteria: 1) it reaches the required tissue compartment, 2) engages the desired target, 3) triggers the desired downstream pharmacological effect. This paper describes the progress made along this track for biologics, in the first instance for monoclonal antibodies, their fragments and therapeutic proteins in general. Cross-species/cross-modality physiologically-based pharmacokinetics (PBPK) framework aims to provide the first principle quantitative predictions for the first two of the declared Pillars. The approach is based on two-pore hypothesis of extravasation, further developed with PBPK in mind and parameterized for fractional tissue lymph flow rates using rodent data. The biologics PBPK framework is validated by accurately predicting the tissue distribution and elimination properties of normal and modified antibodies and their fragments in primate and human studies.

**Keywords:** physiologically-based pharmacokinetics, PBPK, biologics, therapeutic antibodies, therapeutic proteins.

## INTRODUCTION

Although significant progress has been made in cancer care alone with milestone therapeutics in the form of checkpoint inhibitors (Galluzzi et al. 2020) and CAR-T cells (Mikkilineni and Kochenderfer 2021) reaching the clinic, they come at a significant cost with only a fraction of patients benefitting, thus enforcing rationing within constraints of the healthcare resources available. Some of the pressure could be relieved if new therapies were more affordable but, as was very clearly explained recently by Vaiksaar and Käänik (2022), this is easier said than done, given that the income earned from the approved drugs must also cover the development and testing costs of the >90% which fail in clinical trials for various reasons. Once all these bills have been paid, there is not much left over.

The average cost of a new approved drug reaching about a billion dollars also reflects the additional effort required for reaching the 'higher-hanging fruit', which has not been matched with improved likelihood in clinical success rates (Schlander et al. 2021). The reasons for late-stage failures were analysed by Morgan et al. (2012) who formulated the paradigm of 'Three Pillars of Pharmaceutical Survival' to overcome at least some of the inadequacies.

In this review, I describe how these principles can be applied to biologics, e.g. monoclonal antibodies (mAbs), their fragments and therapeutic proteins in general. In a broader sense, the framework is also applicable to any protein, be it dosed or endogenous, thereby expanding the insight into system-level functioning across species from mouse to man.

## PHYSIOLOGICALLY-BASED PHARMACOKINETICS FOR BIOLOGICS

*Large molecule tissue distribution*. It is well known that during the first 3–5 days after intravenous dosing of IgG or albumin, about half of the amount given is lost from the plasma compartment *but remains in the body* (Rossing 1978). The 'missing' fraction becomes extravasated into interstitial space and is found in interstitial fluid (ISF) (Wagner and Wiig 2015) that fills the space between blood vessels and parenchymal cells. ISF takes up around 3/4 of the total of 12 L extracellular fluid volume in humans (Feher 2012), the balance being plasma.

The process of large molecule extravasation involves lymphatic circulation whereby a small fraction of vascular plasma continuously flows under hydrostatic pressure from capillaries into interstitium where it reaches the collecting lymphatics and passes through approximately 500 lymph nodes (in the case of humans) before merging into the venous side of circulation (Swartz 2001; Pavelka and Roth 2010; Swanson and King 2019). In humans, the total lymph flow rate measured in the thoracic duct is about 2–8 L/day, much slower compared with 3.1 L/min cardiac plasma output (Moore Jr. and Bertram 2018) but essential for normal physiology.

*Model formulation.* The quantitative mechanistic framework that relates paracellular plasma flow (and hence, lymph formation rate) to protein extravasation was formulated as a two-pore hypothesis (2PH) by Rippe and Haraldsson (1994) and is based on Patlak formalism (Patlak et al. 1963) whereby the paracellular flux of plasma proteins is characterized by filtration and diffusion. The former component is dictated by the paracellular fluid flow rate and the latter by the concentration gradients. Both are subject to the relative sizes of the paracellular pores and those of the solutes. The paracellular pores have been estimated to be about 5–50 nm in diameter, i.e. approximately the same size as typical plasma proteins (Sarin 2010). The more defined values of 8.9 nm diameter for small pores and 44.5 nm for the large ones, as outlined in Fig. 1, were defined in 2PH reconcile fluid paracellular flow rates with protein paracellular filtration and diffusion. It is understood that the ratio of the pores remains largely invariant throughout the body (small:large at around 6000:1) but their density is organ-dependent, resulting in a different fraction of the incoming plasma flow $Q_{org}$ being diverted to lymphatics at the flow rate $J_{org}$. As protein X enters the vascular space, it becomes subject to a number of processes: there is transport by bulk plasma flow, two-pore exchange with the interstitium and non-specific cellular uptake into the endosomal compartment of endothelial cells (Kup) that represents macropinocytosis. In endosomal space, the proteins which bind the neonatal Fc receptor FcRn can be recycled ($k_{rec}$) back to the cell surface and released into circulation, while the rest are condemned to lysosomal degradation ($k_{deg}$). The fraction of recycling FcRn that ends up in the vascular space is denoted by the coefficient FR, while the rest is destined to interstitium, thus also providing the route to transcytosis.

In summary, all plasma proteins, dosed or endogenous, are subject to filtration and diffusion as they extravasate from plasma to interstitium during blood circulation, with the major ones (albumin, IgG) undergoing around two- to four-fold dilution *en route* (Wiig and Swartz 2012).

*Whole-body physiology*. In biologics PBPK, the default organ structure in Fig. 1 needs to be applied to all organs in the body at the same time according to the way they are connected by blood flows and lymphatics, in order to account for the fate of any dosed endogenous protein, as shown in Fig. 2. All major organs are included and account for >98% of the body mass, with some simplifications and adaptations, as described below. In the case of lungs, the pulmonary circulation accommodates the entire cardiac output, and the outflow is split between the rest of the organs of the body, with 'Heart' denoting cardiac muscle. Most of the organs are connected in parallel, except for the liver, which gets part of its blood supply directly via hepatic artery, with the rest arriving as the venous outflow from gastrointestinal tract, spleen and pancreas.

Both kidneys are combined into one and are supplemented with a compartment that lumps the glomerulus, Bowman's capsule and loops of Henle. The fluid in this space arrives by glomerular filtration from renal vascular compartment, and it empties into bladder at urine formation rate. The latter is about 200-fold slower than the former, thus representing 99.5% reabsorption of water in renal cortex and corresponding to increases in protein concentrations. The glomerular filtration coefficient is treated as a function of protein hydrodynamic radius (i.e. molecular weight) (Sepp et al. 2019), empirically fitted to experimental protein data by Venturoli and Rippe (2005).

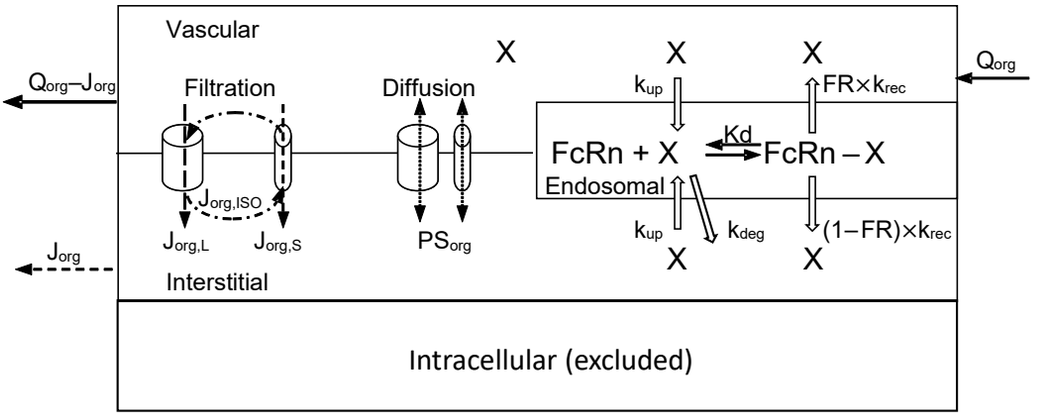


**Fig. 1.** Generic organ layout for biologics showing fluid transfer and protein X transport from the vascular space to the interstitial space through small and large pores according to the two-pore hypothesis. Macropinocytosis, catabolism and FcRn-mediated recycling in the endosomal space are also included, setting the threshold limit values for each pathway. Figure reproduced from Sepp et al. (2019) with permission from Springer (License No. 546713003925).

Lungs contain an alveolar compartment where the epithelial lining fluid (ELF) is in passive protein size-dependent diffusional exchange with interstitium. The absorption of inhaled compounds from the air into ELF is not explicitly modelled and is instead defined as a fraction that reaches the alveolar space. This process is primarily affected by the size distribution of inhaled aerosols, and as little as 10% or less of the inhaled dose may reach ELF, even with dedicated nebulizers being used. Proteins residing in ELF are subject to rapid local non-specific degradation with half-life around 4–8 hours, which severely limits the systemic bioavailability of larger proteins (Sepp et al. 2019; Jagdale et al. 2022). The lung model augmented with alveolar ELF and local exchange kinetic processes allows to evaluate pulmonary and systemic exposure of biologics both from the local and systemic exposure perspectives.

Brain interstitial space has been lumped with cerebrospinal fluid (CSF) (Sepp et al. 2019), while the paracellular two-pore system is supplemented with aquaporin-mediated water flow (Chang et al. 2022b; Wu et al. 2022). The turnover of brain interstitial fluid is taken to be equal to that of CSF and comprises of the sum of aquaporin and two-pore flows. The contribution of paracellular flow is negligible, as dictated by the observed, approximately 300-fold drop in concentration for the main plasma proteins and rapid turnover of brain ISF. The average brain concentration of dosed biologics is thereby nearly fully accounted for by the vascular component within the margin of experimental error, and ISF concentrations are only available with direct *in situ* sampling (Chang et al. 2019; Chang et al. 2022b; Wu et al. 2022).

Solid tumours are very heterogeneous both in terms of cellular composition and spatial organization, but a recurring observation is that they are devoid of functioning lymphatics (Wagner and Wiig 2015) and their vascular porosity is higher than that of normal tissues (Sarin et al. 2009). Within the framework of the model shown in Fig. 1, this means that $J_{org}$ is assigned as zero (Li et al. 2021; Chang et al. 2022a), leaving paracellular diffusion and FcRn-mediated transcytosis as the only routes of extravasation. Both are of low capacity, though; hence tumour penetration can become rate-limiting in the case of cancer cell surface antigens with strong target-mediated drug disposition (TMDD). In such cases, most of the extravasated mAb is internalized and degraded in tumour cell layers close to the capillary walls and does not reach the cells in tumour interior, leaving them underexposed. This is known as antibody affinity barrier (Rudnick and Adams 2009). Mathematical description of the intratumoural antibody concentration gradients can be carried out in terms of partial differential equations (Thurber et al. 2008; Thurber and Wittrup 2008; Wittrup et al. 2012).

Finally, within therapeutic setting, one should also consider subcutaneous (SC) and intramuscular (IM) routes of administration. Whilst intravenous (IV) dosing allows rapid 100% bioavailability, it involves medical assistance and patient inconvenience. On the other hand, the maximum level of SC or IM is more convenient but the dose is limited to about 3 mg/kg due to the maximum injected volume around 1.5 mL and the drug

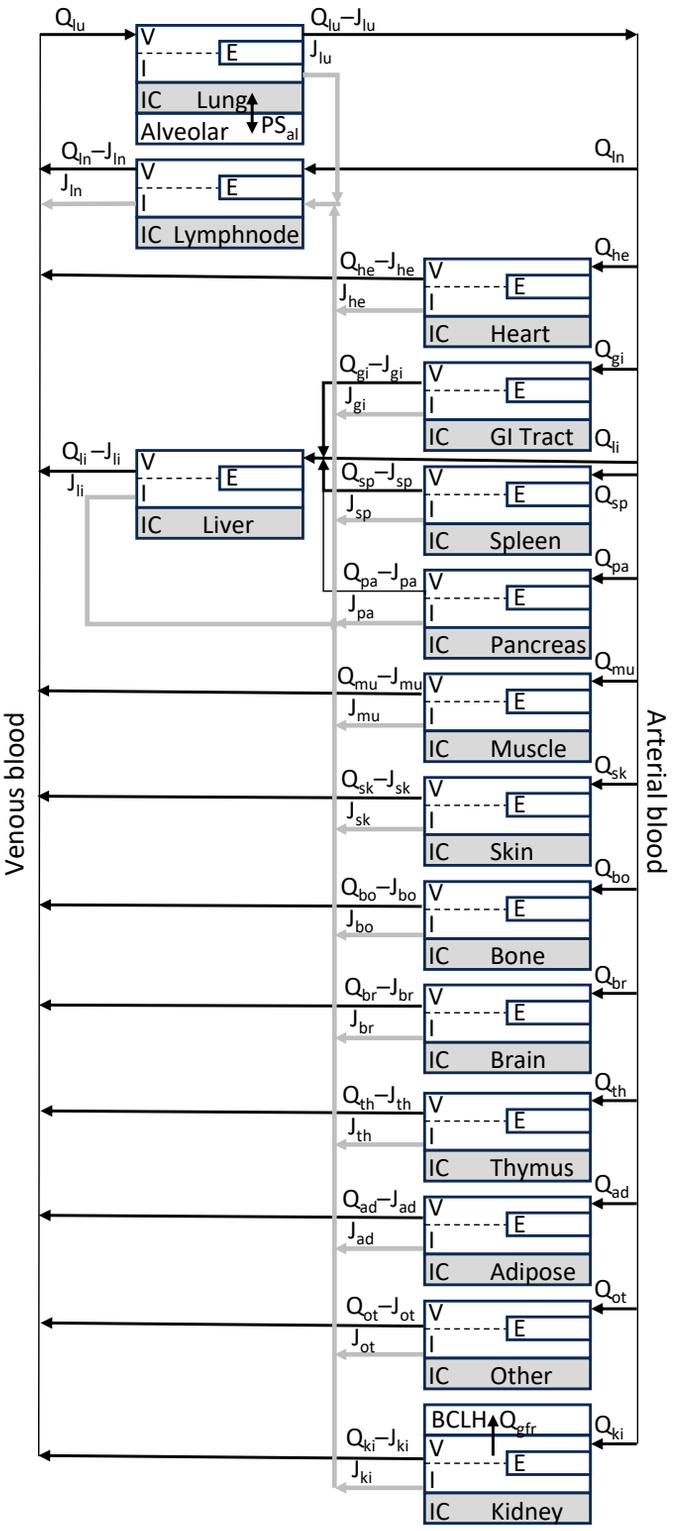


**Fig. 2.** The overall tissue layout of large molecule PBPK is conserved for all mammalian species. In addition to blood circulation, it also contains lymphatic system and distinct vascular (V), interstitial (I), endosomal (E) and, optionally, intracellular (IC, cytoplasm + nucleus, etc.) compartments for each organ. Q – plasma flow, J – lymph flow. The organ-specific adaptations include alveolar space in the lungs and combined glomerulus and loops of Henle (BCLH) in the kidneys. Figure reproduced from Sepp et al. (2019) with permission from Springer (License No. 546713003925).

concentration to 150 mg/mL in the case of mAbs (Viola et al. 2018). In the framework of PBPK, the SC and IV dosing sites are treated as separate from total skin and skeletal muscle compartments, as the dose will not become distributed across the entire organ (Richter and Jacobsen 2014). Depending on the dosed protein size, approximately 100% of the mAb dose is absorbed through lymphatics, whilst being subject to first-pass catabolism in the hematopoietic cells of the draining lymph nodes that results in 60–80% systemic bioavailability (Richter et al. 2018). For smaller proteins like insulin, most of the dose is absorbed into circulation across vasculature and is driven by diffusion. This results in higher bioavailability and quicker absorption (Porter and Charman 2000; Kagan et al. 2012; Kagan and Mager 2013; Richter and Jacobsen 2014).

*Mathematical formalism and model construction*. The two-pore formalism outlined in Fig. 1 needs to be presented within the context of whole-body physiology shown in Fig. 2 and include any drug-specific interactions with endogenous proteins as they may vary from drug to drug. The generic form has been described many times, e.g. by Baxter, Ferl and others (Baxter et al. 1994; Ferl et al. 2005; Gill et al. 2015; Sepp et al. 2015), e.g. by Sepp et al. (Sepp et al. 2019).

$$V_{org,VS}\frac{dC_{org,VS}}{dt} = Q_{org,X}\cdot C_A - \left(Q_{org} - J_{org}\right)\cdot C_{org,VS} - CL_{org}\cdot C_{org,VS} - Kup_{org}\cdot C_{org,VS} + k_{rec}\cdot$$

$$FR\cdot V_{org,EN}\cdot C_{org,EN}^{bound}, \quad (1)$$

$$V_{org,IS}\frac{dC_{org,IS}}{dt} = -J_{org}\cdot C_{org,IS} + CL_{org}\cdot C_{org,VS} - Kup_{org}\cdot C_{org,IS} + k_{rec}\cdot(1-FR)\cdot V_{org,EN}\cdot C_{org,EN}^{bound}, \quad (2)$$

$$V_{org,EN}\frac{C_{org,EN}^{free}}{dt} = Kup_{org}\cdot\left(C_{org,IS} + C_{org,VA}\right) - k_{deg}\cdot V_{org,EN}\cdot C_{org,EN}^{free} - k_{on,FcRn}\cdot V_{org,EN}\cdot$$

$$C_{org,EN}^{free}\cdot C_{org,EN}^{FcRn,free} + k_{off,FcRn}\cdot V_{org,EN}\cdot C_{org,EN}^{FcRn,bound}, \quad (3)$$

$$V_{org,EN}\frac{C_{org,EN}^{bound}}{dt} = V_{org,EN}\cdot k_{on,FcRn}\cdot C_{org,EN}^{free}\cdot C_{org,EN}^{FcRn,free} - V_{org,EN}\cdot k_{off,FcRn}\cdot C_{org,EN}^{FcRn,bound} -$$

$$V_{org,EN}\cdot k_{rec}\cdot C_{org,EN}^{bound}. \quad (4)$$

In Eqs 1–4, $V_{org,VA}$, $V_{org,IS}$ and $V_{org,EN}$ correspond to organ vascular, interstitial and endosomal volumes; $Q_{org}$ represents plasma flow entering the organ and $J_{org}$ lymph flow leaving the organ. $C_A$, $V_{org,VS}$ and $C_{org,IS}$ are drug concentrations in plasma, vascular and interstitial compartments, respectively, while $C_{org,EN}^{free}$ and $C_{org,EN}^{bound}$ denote free and $FcRn$-bound drugs in endosomal compartment, where $C_{org,EN}^{FcRn,free}$ and $C_{org,EN}^{FcRn,bound}$ are free and drug-bound $FcRn$ fractions. $Kup_{org}$ is organ-specific macropinocytosis uptake, $k_{rec}$ the endosomal recycling rate constant and $k_{deg}$ the non-specific endosomal degradation rate constant. $FR$ denotes the fraction of $FcRn$-$mAb$ complex that is recycled to the vascular compartment. $k_{on,FcRn}$ and $k_{off,FcRn}$ denote the association and dissociation rate constants of drug interaction with endosomal $FcRn$. If there are any target-mediated interactions taking place in plasma, interstitial and other compartments, those need to be added accordingly.

Organ-specific two-pore clearance $CL_{org,Y}$ where $Y$ denotes small or large pores

$$CL_{org,Y} = J_{org,Y}\cdot\left(1-\sigma_{org,Y}\right) + PS_{org,Y}\cdot\left(1-\frac{C_{org,IS}}{C_{org,VS}}\right)\cdot\frac{Pe_{org,Y}}{e^{Pe_{org,Y}}-1}, \quad (5)$$

$J_{org,Y}$ denotes the organ-specific small or large pore lymph flow rate, $s_x$ is the reflection coefficient for drug, $PS_{org,Y}$ is permeability-surface area product and $Pe_{org,Y}$ the Peclet coefficient. The first part of the equation describes the filtration flux and the second part the diffusion component.

$J_{org,Y}$ itself combines the total organ flow rate $J_{org}$ with large/small pore hydraulic conductance $a_Y$ and isogravimetric flow $J_{iso,org,Y}$, where the latter is a local transvascular oncotic pressure gradient-driven circulation:

$$J_{org,L} = J_{iso,org} + \alpha_L \cdot J_{org}, \tag{6}$$

$$J_{org,S} = -J_{iso,org} + \alpha_S \cdot J_{org}. \tag{7}$$

Given that both diffusion and filtration fluxes proceed through the same pores at the same time, hence $PS_{org,Y}$ and $J_{iso,org}$ are linear functions of $J_{iso}$, as has been demonstrated by Sepp et al. (2015) and Gill et al. (2015).

All parameters used in Eqs 8–9 are independently measured and reported in literature (Sepp et al. 2015; Sepp et al. 2019), except for the organ-specific lymph flow rates $J_{org}$. These are typically estimated from tissue distribution time course experimental data by calculating the interstitial concentrations from the measured organ average and plasma concentrations (Sepp et al. 2019).

$$PS_{org,Y} = \frac{8 \cdot R \cdot T}{6\pi \cdot N \cdot a_e \cdot (\Delta P - \overline{\sigma}_{org,alb} \cdot \Delta\pi)} \cdot \left(\frac{A_Y}{A_{oY}}\right)_{org} \cdot \frac{\alpha_{org,Y}}{r^2_{org,Y}} \cdot J_{org}, \tag{8}$$

$$J_{iso,org} = \frac{\alpha_{L,org} \cdot \alpha_{S,org} \cdot (\sigma_{S,org,alb} - \sigma_{L,org,alb}) \cdot \Delta\pi}{6\pi \cdot N \cdot a_e \cdot (\Delta P - \overline{\sigma}_{org,alb} \cdot \Delta\pi)} \cdot J_{org}. \tag{9}$$

Until this day, most pharmacokinetic models are manually coded in graphical or text editor environments (Ferl et al. 2005; Shah and Betts 2012; Gill et al. 2015; Sepp et al. 2015). Needless to say, the number of differential equations and supporting algebraic expressions rises rapidly as the models get more complex and, soon enough, the time and effort involved becomes prohibitive. This limitation was overcome with the introduction of computer-assisted coding of biologic PBPK models fit for simulation and parameter estimation in Matlab SimBiology environment (Sepp et al. 2019). For example, it requires less than two minutes to build a model containing 3364 differential and algebraic equations to describe the tissue distribution and elimination kinetics of endogenous and dosed albumin and IgG, dosed antibody fragment and its complex with albumin, as well as all relevant complexes with FcRn. By hand this would be impossible for practical purposes because of time and effort required for model coding and debugging. Using computer-assisted model coding, it is now possible to build predictive and mechanistic quantitative models that can describe tissue distribution kinetics and the elimination of any circulating protein with formalism that also extends to membrane-linked proteins, cellular entities and any reactions between them. The overall implementation meets the requirements of the first two of the Three Pillars of Survival, while the last one can be implemented in the form of generic empirical pharmacodynamic function or mechanistic representations, e.g. as a quantitative systems pharmacology (QSP) model.

## DISCUSSION

Most biologic drugs are of recombinant origin, i.e. proteins produced under controlled conditions in genetically engineered eukaryotic cell lines to meet the stringent criteria of reproducibility. Just like endogenous proteins, from the perspective of physicochemical properties that determine their absorption, distribution, metabolism and elimination (ADME), they are often heterogenous, mostly highly charged and polar, with molecular weight that can vary from as low as a few kDa to more than a hundred. Any notion of logP, calculated or experimental, is therefore irrelevant as proteins do not dissolve in organic solvents. Lipinski's

rules of five (Lipinski et al. 2001) that guide the development of small molecule therapeutics to ensure their intracellular availability do not extend to biologics. The ADME properties also shape the respective target repertoires for small and large molecule drugs. Small molecule drugs are mostly used as inhibitors, agonists and antagonists, designed to fit into the active sites of their intra- or extracellular target proteins, while biologics like mAbs predominantly function as competitive inhibitors of protein-protein interactions that take place between receptors and their respective soluble or membrane-bound ligands in extracellular space only (Wells and McClendon 2007). Although much effort has been dedicated towards intracellular delivery of biologics by many different means (Suhorutsenko et al. 2011; Slastnikova et al. 2018), *in vitro* to *in vivo* translation has proven elusive, with cellular specificity, payload impact, uptake levels and endosomal escape remaining the obstacles to overcome.

Two-pore biologics cross-species/cross-modality PBPK presented in Figs 1 and 2, then formalised in Eqs 1–9, was parameterized for the organ-specific fractional lymph flow rates by Sepp et al. (2019), using rodent tissue distribution time course data using a number of test proteins with no known interaction partners. Remarkably, these organ-specific parameters derived from rodent data allowed correct extrapolation to monkeys and humans, as revealed by positron emission tomography (PET) studies of two mAbs and a mAb fragment in these species. In the study by Aweda et al. (2022), we looked at the relative and absolute tissue concentration levels of sotrovimab, a COVID-19 neutralizing mAb with a half-life extending Fc modification and its wild-type parent molecule in monkeys. As predicted by the model and confirmed by the experiment, the FcRn-binding activity does not affect extravasation kinetics or the steady state of mAbs, which enables mechanistic insight into mAb exposure at lung ELF, the first tissue compartment that the inhaled virus meets in the body. Any enhanced exposure to the dosed mAb in tissue interstitial and lung ELF solely arises as a consequence of the extended plasma half-life of antibodies with higher affinity for FcRn at acidic pH values, while the impact of transcytosis is negligible.

In the case of humans, we followed the time course of tissue distribution and penetration of an albumin-binding domain antibody (Fig. 3) (Thorneloe et al. 2019; Sepp et al. 2020). Just as in the case of monkeys,

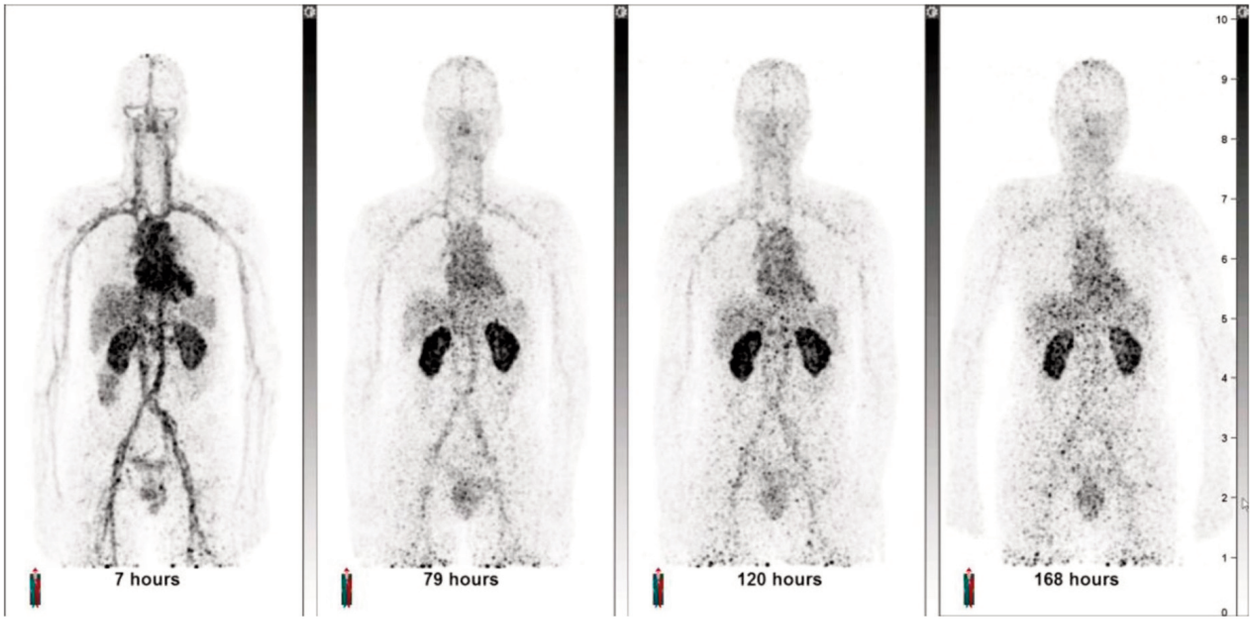


**Fig. 3.** Maximum intensity projections (MIP) of $^{89}$Zr-labelled AlbudAb in humans, obtained at different time points after administration for one representative subject in study (Thorneloe et al. 2019; Sepp et al. 2020). The dose is initially confined to the peripheral blood, as seen in major blood vessels and heart at the first image, gradually distributing elsewhere over 3–4 days. Renal signal is most likely caused by about 1% of the $^{89}$Zr label being unbound in the dosed sample. Figure reproduced from Thorneloe et al. (2019) with permission from Springer (Creative Commons CC BY).

the rodent data parameterized model correctly predicted the human results, thus confirming the cross-species functionality of the approach. The study also exemplified the usefulness of mathematical modelling in study design, given that the healthy volunteers involved could only be exposed to low dose of combined radiation from the radiolabelled $^{89}$Zr-labelled drug and the accompanying computer tomography for imaging purposes.

Finally, the biologics PBPK model presented can also support the third pillar of pharmaceutical survival, i.e. downstream pharmacology that follows from target engagement. Specifically, we demonstrated how the clinically approved dosing cycles of ravulizumab and ibalizumab are related to their respective molecular properties and complex pharmacology (Sepp et al. 2020). Specifically, this involved accounting the affinity changes of the mAbs at neutral and acidic pH values for human complement factor C5 in the context of plasma concentration and turnover of the target and the enhanced affinity of ravulizumab for FcRn. The resulting model demonstrated from the first principles why the latter was superior to eculizumab and how the model could have been used to guide the discovery process. The model for CD4-neutralizing antibody ibalizumab demonstrated how antibody tissue distribution and target engagement can be affected by the properties of the target. It is well known that only around 2% of lymphocytes are present in peripheral blood at any time (Westermann and Pabst 1992), while the rest are predominantly found in secondary lymphoid organs where the mAb availability can be severely limited due to the combination of slow lymph flow rate and rapid target-mediated internalization/degradation on CD4-positive cells. As a result, the concentration of free ibalizumab in lymph nodes can be at least a hundred-fold lower than in plasma, hence explaining why the clinically adjusted dosing regimen aims for the antibody plasma concentration in 10 000-fold excess over the Kd and $IC_{50}$ values of the drug.

## CONCLUSIONS

Fundamentally, the framework presented divides the parameters used for biologics PBPK into several categories. These range from fundamental constants including Avogadro number and absolute temperature to organ-specific physiological constants in the first instance. Some of the latter can be measured, e.g. volumes and blood flow rates, while some need to be estimated indirectly, e.g. lymph flow rates. Once defined, they remain invariant from then on. The drug-related parameters remain largely invariant within class, there is relatively little change from one antibody to another in terms of biophysical properties and size, hence their underlying pharmacokinetic properties are very similar (Betts et al. 2018), and this holds across species from mice to humans (Shah and Betts 2013). In other words, a human mAb with a wild-type sequence outside the paratope region typically displays in humans around 17–20 day terminal half-life, usually unperturbed by soluble targets. If this value is substantially shorter and especially significantly time and concentration-dependent, this indicates the impact of target-mediated elimination which is saturable, varies from one molecule to another according to affinity, tissue distribution, turnover, etc. These are the third kind of parameters in biologics PBPK, the ones that define interactions with one or more targets, which can be soluble, membrane bound, interact with other proteins, etc. This is also the major differentiating factor between large and small molecule PBPK. Target-mediated interactions do not affect the pharmacokinetics of small molecule drugs. The differences observed are due to differential tissue uptake, clearance and elimination through various transporters and cytochrome P-450 enzymes which, in turn, have no impact on large molecule behaviour. While small molecule tissue distribution can often be adequately understood in terms of equilibrium thermodynamics, for biologics the plasma and tissue steady state (if reached) concentrations represent the interplay of flow, filtration, diffusion and interactions with the target.

Drug discovery is a field that brings together the latest in science and immediately puts it to test through practice, sometimes extrapolating beyond the data and insight available. Any misconceptions are sooner or later revealed as failures in the clinic. Mathematical modelling can be useful for providing mechanistic predictive insight into some aspects of these non-linear interconnected processes in complex *in vivo* environments. The benefits can be manifold. Firstly, early modelling and simulation can identify unrealistic expectations and gaps of knowledge before much money and time is spent on them. Beyond that, it can

provide the framework that guides the research and development process itself. Finally, the cross-species/cross-modality framework PBPK for biologics can also support basic science by providing system insight into complex physiological processes and laying the ground rules of how endogenous proteins, cells and other modalities can interact and function both in health and disease.

## ACKNOWLEDGEMENT

The publication costs of this article were partially covered by the Estonian Academy of Sciences.

Photo: private collection

*Armin Sepp is a Senior Principal Scientist at Certara Ltd, where he leads the Biologics section of the Science team, specializing in the physiologically-based pharmacokinetics (PBPK) of biologics. His background in bioorganic chemistry and a PhD in enzyme kinetics from the University of Tartu under the supervision of Prof. Jaak Järv provided the perfect foundation for post-doctoral training in protein engineering and* in vitro *evolution at the MRC Immunochemistry Unit in Oxford and MRC Laboratory of Molecular Biology in Cambridge. Pharmaceutical work started with human domain antibody engineering at Domantis Ltd start-up in Cambridge, followed by GlaxoSmithKline plc (GSK), where he became Scientific Leader and GSK Fellow at the DMPK Modelling group. At GSK, he established a quantitative mechanistic full-body modelling platform for dosed and endogenous proteins, which supported drug discovery projects for mAbs, antibody fragments and other biologics across all therapy areas ranging from immunoinflammation to oncology and gene therapy. In his current job, the focus remains on cross-platform/cross-species PBPK of protein therapeutics, but he is also keeping a keen eye on the developments in the field of machine learning and quantitative systems pharmacology.*

## REFERENCES

Aweda, T. A., Cheng, S.-H., Lenhard, S. C., Sepp, A., Skedzielewski, T., Hsu, C.-Y. et al. 2023. In vivo biodistribution and pharmacokinetics of sotrovimab, a SARS-CoV-2 monoclonal antibody, in healthy cynomolgus monkeys. *Eur. J. Nucl. Med. Mol. Imaging*, **50**, 667–678.

Baxter, L. T., Zhu, H., Mackensen, D. G. and Jain, R. K. 1994. Physiologically based pharmacokinetic model for specific and nonspecific monoclonal antibodies and fragments in normal tissues and human tumor xenografts in nude mice. *Cancer Res.*, **54**(6), 1517–1528.

Betts, A., Keunecke, A., van Steeg, T. J., van der Graaf, P. H., Avery, L. B., Jones, H. et al. 2018. Linear pharmacokinetic parameters for monoclonal antibodies are similar within a species and across different pharmacological targets: a comparison between human, cynomolgus monkey and hFcRn Tg32 transgenic mouse using a population-modeling approach. *mAbs.*, **10**(5), 751–764. https://doi.org/10.1080/19420862.2018.1462429

Chang, H.-P., Li, Z. and Shah, D. K. 2022. Development of a physiologically-based pharmacokinetic model for whole-body disposition of MMAE containing antibody-drug conjugate in mice. *Pharm. Res.*, **39**(1), 1–24. https://doi.org/10.1007/s11095-021-03162-1

Chang, H.-Y., Wu, S., Meno-Tetang, G. and Shah, D. K. 2019. A translational platform PBPK model for antibody disposition in the brain. *J. Pharmacokinet. Pharmacodyn.*, **46**(4), 319–338. https://doi.org/10.1007/s10928-019-09641-8

Chang, H.-Y., Wu, S., Li, Y., Guo, L., Li, Y. and Shah, D. K. 2022. Effect of the size of protein therapeutics on brain pharmacokinetics following systematic administration. *AAPS J.*, **24**(3), 62. https://doi.org/10.1208/s12248-022-00701-5

Feher, J. 2012. Regulation of arterial pressure. In *Quantitative Human Physiology*. Boston, Academic Press, 538–548.

Ferl, G. Z., Wu, A. M. and DiStefano, J. J. III. 2005. A predictive model of therapeutic monoclonal antibody dynamics and regulation by the neonatal Fc receptor (FcRn). *Ann. Biomed. Eng.*, **33**(11), 1640–1652. https://doi.org/10.1007/s10439-005-7410-3

Galluzzi, L., Humeau, J., Buqué, A., Zitvogel, L. and Kroemer, G. 2020. Immunostimulation with chemotherapy in the era of immune checkpoint inhibitors. *Nat. Rev. Clin. Oncol.*, **17**(12), 725–741. https://doi.org/10.1038/s41571-020-0413-z

Gill, K. L., Gardner, I., Li, L. and Jamei, M. 2016. A bottom-up whole-body physiologically based pharmacokinetic model to mechanistically predict tissue distribution and the rate of subcutaneous absorption of therapeutic proteins. *AAPS J.*, **18**(1), 156–170. https://doi.org/10.1208%2Fs12248-015-9819-4

Jagdale, P., Sepp, A. and Shah, D. K. 2022. Physiologically-based pharmacokinetic model for pulmonary disposition of protein therapeutics in humans. *J. Pharmacokinet. Pharmacodyn.*, **49**(6), 607–624. https://doi.org/10.1007/s10928-022-09824-w

Kagan, L. and Mager, D. E. 2013. Mechanisms of subcutaneous absorption of rituximab in rats. *Drug Metab. Dispos.*, **41**(1), 248–255. https://doi.org/10.1124/dmd.112.048496

Kagan, L., Turner, M. R., Balu-Iyer, S. V. and Mager, D. E. 2012. Subcutaneous absorption of monoclonal antibodies: role of dose, site of injection, and injection volume on rituximab pharmacokinetics in rats. *Pharm. Res.*, **29**(2), 490–499. https://doi.org/10.1007/s11095-011-0578-3

Li, Z., Li, Y., Chang, H. P., Yu, X. and Shah, D. K. 2021. Two-pore physiologically based pharmacokinetic model validation using whole-body biodistribution of trastuzumab and different-size fragments in mice. *J. Pharmacokinet. Pharmacodyn.*, **48**(6), 743–762. https://doi.org/10.1007/s10928-021-09772-x

Lipinski, C. A., Lombardo, F., Dominy, B. W. and Feeney, P. J. 2001. Experimental and computational approaches to estimate solubility and permeability in drug discovery and development settings. *Adv. Drug Deliv. Rev.*, **46**(1–3), 3–26. https://doi.org/10.1016/s0169-409x(00)00129-0

Mikkilineni, L. and Kochenderfer, J. N. 2021. CAR T cell therapies for patients with multiple myeloma. *Nat. Rev. Clin. Oncol.*, **18**(2), 71–84. https://doi.org/10.1038/s41571-020-0427-6

Moore, J. E., Jr. and Bertram, C. D. 2018. Lymphatic system flows. *Annu. Rev. Fluid Mech.*, **50**, 459–482. https://doi.org/10.1146/annurev-fluid-122316-045259

Morgan, P., Van Der Graaf, P. H., Arrowsmith, J., Feltner, D. E., Drummond, K. S., Wegner, C. D. et al. 2012. Can the flow of medicines be improved? Fundamental pharmacokinetic and pharmacological principles toward improving Phase II survival. *Drug Discov. Today*, **17**(9–10), 419–424. https://doi.org/10.1016/j.drudis.2011.12.020

Patlak, C. S., Goldstein, D. A. and Hoffman, J. F. 1963. The flow of solute and solvent across a two-membrane system. *J. Theor. Biol.*, **5**(3), 426–442. https://doi.org/10.1016/0022-5193(63)90088-2

Pavelka, M. and Roth, J. 2010. Fluid-phase endocytosis and phagocytosis. In *Functional Ultrastructure: Atlas of Tissue Biology and Pathology*. Springer, Vienna, 104–105.

Porter, C. J. and Charman, S. A. 2000. Lymphatic transport of proteins after subcutaneous administration. *J. Pharm. Sci.*, **89**(3), 297–310. https://doi.org/10.1002/(sici)1520-6017(200003)89:3%3C297::aid-jps2%3E3.0.co;2-p

Richter, W. F. and Jacobsen, B. 2014. Subcutaneous absorption of biotherapeutics: knowns and unknowns. *Drug Metab. Dispos.*, **42**(11), 1881–1889. https://doi.org/10.1124/dmd.114.059238

Richter, W. F., Christianson, G. J., Frances, N., Grimm, H. P., Proetzel, G. and Roopenian, D. C. 2018. Hematopoietic cells as site of first-pass catabolism after subcutaneous dosing and contributors to systemic clearance of a monoclonal antibody in mice. *mAbs.*, **10**(5), 803–813. https://doi.org/10.1080/19420862.2018.1458808

Rippe, B. and Haraldsson, B. 1994. Transport of macromolecules across microvascular walls: the two-pore theory. *Physiol. Rev.*, **74**(1), 163–219. https://doi.org/10.1152/physrev.1994.74.1.163

Rossing, N. 1978. Intra- and extravascular distribution of albumin and immunoglobulin in man. *Lymphology*, **11**(4), 138–142.

Rudnick, S. I. and Adams, G. P. 2009. Affinity and avidity in antibody-based tumor targeting. *Cancer Biother. Radiopharm.*, **24**(2), 155–161. https://doi.org/10.1089/cbr.2009.0627

Sarin, H. 2010. Physiologic upper limits of pore size of different blood capillary types and another perspective on the dual pore theory of microvascular permeability. *J. Angiogenes. Res.*, **2**(1), 14. https://doi.org/10.1186/2040-2384-2-14

Sarin, H., Kanevsky, A. S., Wu, H., Sousa, A. A., Wilson, C. M., Aronova, M. A. et al. 2009. Physiologic upper limit of pore size in the blood-tumor barrier of malignant solid tumors. *J. Transl. Med.*, **7**, 51. https://doi.org/10.1186/1479-5876-7-51

Schlander, M., Hernandez-Villafuerte, K., Cheng, C.-Y., Mestre-Ferrandiz, J. and Baumann, M. 2021. How much does it cost to research and develop a new drug? A systematic review and assessment. *PharmacoEconomics*, **39**(11), 1243–1269. https://doi.org/10.1007/s40273-021-01065-y

Sepp, A., Berges, A., Sanderson, A. and Meno-Tetang, G. 2015. Development of a physiologically based pharmacokinetic model for a domain antibody in mice using the two-pore theory. *J. Pharmacokinet. Pharmacodyn.*, **42**(2), 97–109. https://doi.org/10.1007/s10928-014-9402-0

Sepp, A., Meno-Tetang, G., Weber, A., Sanderson, A., Schon, O. and Berges, A. 2019. Computer-assembled cross-species/cross-modalities two-pore physiologically based pharmacokinetic model for biologics in mice and rats. *J. Pharmacokinet. Pharmacodyn.*, **46**(4), 339–359. https://doi.org/10.1007/s10928-019-09640-9

Sepp, A., Bergström, M. and Davies, M. 2020. Cross-species/cross-modality physiologically based pharmacokinetics for biologics: 89Zr-labelled albumin-binding domain antibody GSK3128349 in humans. *mAbs.*, **12**(1), 1832861. https://doi.org/10.1080/19420862.2020.1832861

Shah, D. K. and Betts, A. M. 2012. Towards a platform PBPK model to characterize the plasma and tissue disposition of monoclonal antibodies in preclinical species and human. *J. Pharmacokinet. Pharmacodyn.*, **39**(1), 67–86. https://doi.org/10.1007/s10928-011-9232-2

Shah, D. K. and Betts, A. M. 2013. Antibody biodistribution coefficients: inferring tissue concentrations of monoclonal antibodies based on the plasma concentrations in several preclinical species and human. *mAbs.*, **5**(2), 297–305. https://doi.org/10.4161/mabs.23684

Slastnikova, T. A., Ulasov, A. V., Rosenkranz, A. A. and Sobolev, A. S. 2018. Targeted intracellular delivery of antibodies: the state of the art. *Front. Pharmacol.*, **9**. https://doi.org/10.3389/fphar.2018.01208

Suhorutsenko, J., Oskolkov, N., Arukuusk, P., Kurrikoff, K., Eriste, E., Copolovici, D. M. et al. 2011. Cell-penetrating peptides, PepFects, show no evidence of toxicity and immunogenicity in vitro and in vivo. *Bioconjug. Chem.*, **22**(11), 2255–2262. https://doi.org/10.1021/bc200293d

Swanson, J. A. and King, J. S. 2019. The breadth of macropinocytosis research. *Philos. Trans. R. Soc. Lond. B. Biol. Sci.*, **374**(1765), 20180146. https://doi.org/10.1098/rstb.2018.0146

Swartz, M. A. 2001. The physiology of the lymphatic system. *Adv. Drug Deliv. Rev.*, **50**(1–2), 3–20. https://doi.org/10.1016/s0169-409x(01)00150-8

Thorneloe, K. S., Sepp, A., Zhang, S., Galinanes-Garcia, L., Galette, P., Al-Azzam, W. et al. 2019. The biodistribution and clearance of AlbudAb, a novel biopharmaceutical medicine platform, assessed via PET imaging in humans. *EJNMMI Res.*, **9**(1), 45. https://doi.org/10.1186/s13550-019-0514-9

Thurber, G. M. and Wittrup, K. D. 2008. Quantitative spatiotemporal analysis of antibody fragment diffusion and endocytic consumption in tumor spheroids. *Cancer Res.*, **68**(9), 3334–3341. https://doi.org/10.1158/0008-5472.can-07-3018

Thurber, G. M., Schmidt, M. M. and Wittrup, K. D. 2008. Antibody tumor penetration: transport opposed by systemic and antigen-mediated clearance. *Adv. Drug Deliv. Rev.*, **60**(12), 1421–1434. https://doi.org/10.1016/j.addr.2008.04.012

Vaiksaar, R. and Käänik, J. 2022. Millest tulenevad vähiravimite hirmkallid hinnad? (Origin of over-the-top prices of cancer drugs). https://www.delfi.ee/artikkel/120118518/selgitav-video-21-000-eurot-41-000-eurot-millest-tulenevad-vahiravimite-hirmkallid-hinnad (accessed 2023-02-10).

Venturoli, D. and Rippe, B. 2005. Ficoll and dextran vs. globular proteins as probes for testing glomerular permselectivity: effects of molecular size, shape, charge, and deformability. *Am. J. Physiol. Renal Physiol.*, **288**(4), F605–F613. https://doi.org/10.1152/ajprenal.00171.2004

Viola, M., Sequeira, J., Seiça, R., Veiga, F., Serra, J., Santos, A. C. et al. 2018. Subcutaneous delivery of monoclonal antibodies: how do we get there? *J. Control. Release,* **286**, 301–314. https://doi.org/10.1016/j.jconrel.2018.08.001

Wagner, M. and Wiig, H. 2015. Tumor interstitial fluid formation, characterization, and clinical implications. *Front. Oncol.,* **5**, 115. https://doi.org/10.3389/fonc.2015.00115

Wells, J. A. and McClendon, C. L. 2007. Reaching for high-hanging fruit in drug discovery at protein–protein interfaces. *Nature*, **450**, 1001–1009.

Westermann, J. and Pabst, R. 1992. Distribution of lymphocyte subsets and natural killer cells in the human body. *Clin. Investig.*, **70**(7), 539–544. https://doi.org/10.1007/bf00184787

Wiig, H. and Swartz, M. A. 2012. Interstitial fluid and lymph formation and transport: physiological regulation and roles in inflammation and cancer. *Physiol. Rev.*, **92**(3), 1005–1060. https://doi.org/10.1152/physrev.00037.2011

Wittrup, K. D., Thurber, G. M., Schmidt, M. M. and Rhoden, J. J. 2012. Practical theoretic guidance for the design of tumor-targeting agents. *Methods Enzymol*., **503**, 255–268. https://doi.org/10.1016/b978-0-12-396962-0.00010-0

Wu, S., Le Prieult, F., Phipps, C. J., Mezler, M. and Shah, D. K. 2022. PBPK model for antibody disposition in mouse brain: validation using large-pore microdialysis data. *J. Pharmacokinet. Pharmacodyn.*, **49**(6), 579–592. https://doi.org/10.1007/s10928-022-09823-x

## Bioloogiliste makromolekulide füsioloogiline farmakokineetika

Armin Sepp

Ravimiarendus on valdkond, mis ühelt poolt toetub tippteadusele ning teisalt mõjutab sümbiootiliselt ka selle prioriteete ja arengut. Bioloogiliste ravimite füsioloogiline farmakokineetika on valdkond, mis juhatab sisse kvantitatiivse, mehhanistliku (*predictive*) temaatika ravimiarenduse metoodikas ning loob ka tugiraamistiku, millele toetudes saab fundamentaalteaduse võtmes analüüsida organismi erinevate osade funktsioneerimist ühtse tervikuna, seda nii normaalses kui ka patoloogilises füsioloogilises kontekstis.